Human Reproduction vol.15 no.12 pp.2621–2633, 2000

Differential mitochondrial distribution in human pronuclear embryos leads to disproportionate inheritance between blastomeres: relationship to microtubular organization, ATP content and competence

Jonathan Van Blerkom[1,2,3], Patrick Davis[1,2] and Samuel Alexander[2]

[1]Department of Molecular, Cellular and Developmental Biology, University of Colorado, Boulder, CO 80302 and [2]Colorado Reproductive Endocrinology, Rose Medical Center, Denver, CO, 80220, USA

[3]To whom correspondence should be addressed at: Department of Molecular, Cellular and Developmental Biology, University of Colorado, Boulder, CO 80302, USA
E-mail: vanblerk@spot.colorado. edu

It has been suggested that mitochondrial DNA defects that effect metabolic capacity may be a proximal cause of failures in oocyte maturation, fertilization, or early embryonic development. Here, the distribution of mitochondria was examined by scanning laser confocal microscopy in living human pronuclear oocytes and cleavage stage embryos, followed either by measurements of the net ATP content of individual blastomeres or anti-tubulin immunofluorescence to determine the relationship between mitochondrial distribution and microtubular organization. The results indicate that specific patterns of perinuclear mitochondrial aggregation and microtubular organization are related, and that asymmetrical mitochondrial distributions at the pronuclear stage can result in some proportion of blastomeres with reduced mitochondrial inheritance and diminished ATP generating capacity. While the inability to divide appears to be a development consequence for an affected blastomere, for the embryo, reduced competence may occur during cleavage if several blastomeres inherit a mitochondrial complement inadequate to support normal cellular functions. The findings provide a possible epigenetic explanation for the variable developmental ability expressed within cohorts of morphologically normal early cleavage stage human embryos obtained by in-vitro fertilization.

Key words: cleavage stage embryos/metabolism/mitochondria/microtubules/pronuclear embryos

Introduction

Outcomes from clinical IVF demonstrate that each embryo has a unique developmental potential. Embryo-specific competence is most often evident during the cleavage stages where some proportion of embryos within cohorts arrest cytokinesis or progress in culture in a manner that is stage-inappropriate with respect to cell number (developmentally delayed). The temporal origins and specific causes of developmental failure or delay can be difficult to determine in a clinical setting because embryos available for experimental analysis are usually those 'de-selected' for transfer or cryopreservation because of extensive fragmentation. However, recent evidence suggests that physiological factors within the pre-ovulatory follicle and the specificity and pattern of cellular processes that occur shortly after fertilization can have downstream consequences for development. For example, perifollicular vascularity and intrafollicular biochemistry are follicle-specific characteristics that have been related to chromosomal normality for the oocyte (Van Blerkom *et al*., 1997), embryo competence during cleavage (Huey *et al*., 1999), and outcome after embryo transfer (Coulam *et al*., 1999; Gregory *et al*., 1999). Specific characteristics of nuclear and cytoplasmic organization detected within and between cohorts of pronuclear-stage human oocytes have been related to outcome after IVF. For example, an equatorial alignment of nucleoli at the region of pronuclear opposition has been reported to be an early sign of developmental competence (Scott and Smith, 1998; Tesarik and Greco, 1999). The appearance of a subplasmalemmal zone of translucent cytoplasm observed as a focal clearing within the cortical cytoplasm (cytoplasmic flare; Payne *et al*., 1997), which often progresses to involve the entire cytocortex (pronuclear halo; Scott and Smith, 1998), as well as the spatial orientation of pronuclei with respect to the polar bodies (Garello *et al*., 1999), have been reported to be clinically significant indicators of developmental potential during the preimplantation stages and of competence after transfer.

Here, it is investigated whether spatial differences in the organization of mitochondria at the pronuclear stage may be another developmentally significant characteristic of early human embryos that may determine competence. Preliminary studies of mitochondrial segregation between blastomeres in 2-4-cell human embryos (conventional IVF) demonstrated disproportionate patterns of mitochondrial inheritance (Van Blerkom, 2000). In cases where most mitochondria were partitioned into one blastomere, the deficient blastomere remained undivided and lysed during subsequent culture. In the present study, the objectives were to determine (i) whether differences in mitochondrial distribution occurred among individual blastomeres in cohorts of morphologically normal (unfragmented) cleavage stage embryos derived from 'high-competence' pronuclear oocytes, (ii) whether differences in mitochondrial inheritance were related to blastomere ATP content, and (iii) whether a cytoarchitectural basis for specific

patterns of mitochondrial organization existed at the pronuclear stage.

Materials and methods

Pronuclear oocytes and cleavage stage embryos

Pronuclear oocytes and cleavage stage embryos were obtained from women between 25 and 37 years of age undergoing conventional IVF after gonadotrophin-releasing hormone (GnRH) suppression and ovarian suppression and ovulation induction as previously described (Van Blerkom *et al*., 1995a). None of the embryos described in this study involved a male factor. According to protocol, unpenetrated monopronuclear oocytes and dispermic oocytes/embryos were available for analysis, and monospermic oocytes/embryos were donated to research. Fluorescent staining of DNA (DAPI), mitochondria [rhodamine 123 (R123) for metabolically active mitochondria; noracridine orange (NAO) for all mitochondria regardless of activity (Van Blerkom *et al*., 1998)], and immunofluorescent detection of microtubules (Van Blerkom *et al*., 1995a) followed procedures previously described. Monopronuclear oocytes were classified as unpenetrated owing to the absence of a sperm nucleus as determined by DAPI staining (Van Blerkom *et al*., 1994). The failure of penetration was confirmed during immunofluorescent analysis by the absence of a sperm head and tail. Disaggregation of cleavage stage embryos into component blastomeres was accomplished by a brief (15–20 s) exposure to acidic Tyrode's solution followed by manual dissection of the zona pellucida with glass microneedles in calcium- and magnesium-free phosphate-buffered saline. Blastomeres were removed individually from the embryo by means of a micropipette.

Microscopic analysis

Here, the analysis was confined to pronuclear oocytes (and resulting embryos) that, at 16-18 h after insemination, showed an equatorial nucleolar alignment and an unambiguous cytoplasmic flare or pronuclear halo, morphological characteristics that have been suggested to indicate high developmental competence. Analysis of mitochondrial fluorescence in living specimens used scanning laser confocal microscopy (SLCM) with temperature and atmosphere maintained during observation in DT culture dishes (Bioptechs, Inc., Butler, PA, USA) as previously described (Van Blerkom *et al*., 1995a). Research protocols that included patient consents permitted two types of analyses to be undertaken for normally fertilized oocytes: (i) analysis during the pronuclear stages up to syngamy and (ii) maintenance of embryos for up to 5 days *in vitro*. In the first case, appropriate pronuclear oocytes were stained with either R123 or NAO and examined in detail by SLCM through syngamy. After SLCM examination, specimens were fixed in formaldehyde, prepared for anti-b-tubulin immunofluorescence, and re-examined by SLCM. In the second case, which also included dispermic oocytes, stained specimens were observed at 16-18 h intervals from the pronuclear to the 16-cell stage. Unpenetrated, monopronuclear oocytes were examined at 16-18 h after insemination and subsequently fixed for immunostaining. Scans of pronuclear oocytes involved serial optical sections taken at intervals of 5 μm, which required 3.5 min to complete. Subsequent analyses of R123 or NAO fluorescence in intact cleavage stage embryos involved sections taken at intervals of 10 μm and <1 min to complete. After disaggregation, individual blastomeres used for ATP analysis were re-scanned to confirm relative intensities of fluorescence observed in the intact embryo. Representative intact embryos were fixed for anti-b-tubulin immunofluorescence. Analysis of mitochondrial and microtubular fluorescence used both serial sections and fully complied images, with blastomere nuclear and cytoplasmic volumes determined from digital images using ImageSpace software (v.3.10, Molecular Dynamics, Sunnyvale, CA, USA). Pseudo-colour images produced by SLCM were generated from specimens examined at the same photomultiplier detector gain and are presented as observed. The colour bar included in the figures represents the spectrum of fluorescence detected (lowest = blue, highest = white) with numerical values (relative fluorescent units) from 0 to 255 indicated.

ATP content

Individual blastomeres were rapidly frozen to –80°C in 200 ml of ultrapure water. ATP content was determined quantitatively by measurement of the luminescence (Berthold LB 9501 luminometer) generated in an ATP-dependent luciferin-luciferase bioluminescence assay as previously described (Van Blerkom *et al*., 1995b). A standard curve containing 14 ATP concentrations from 5 fmol/l to 5 pmol/l was generated for each series of analyses. To reduce potential variability between samples, blastomeres from different embryos were maintained at –80°C and analysed simultaneously. The ATP content in aliquots of selected blastomeres was determined both within and between bioluminescence assays.

Results

The distribution and relative intensity of mitochondrial fluorescence was examined in the living specimens with two mitochondrial membrane probes: R123, which stains active mitochondria, or NAO, which stains active and inactive mitochondria (Van Blerkom and Runner, 1984; Barnett *et al*., 1996). For sequential staining of embryos selected for immunofluorescence analysis, specimens were first stained with R123 and subsequently with NAO; mitochondrial NAO fluorescence persists after fixation. For pronuclear oocytes, light microscopic inspections were performed at 14–16 h after insemination to determine nucleolar organization and the extent and pattern of cortical clearing. Pronuclear oocytes, intact cleavage stage embryos and individual blastomeres after disaggregation were examined as optical sections by SLCM. Based on cytoplasmic appearance observed by light microscopy (e.g. Figure 1A, F), the distribution and relative intensity of mitochondrial fluorescence between and within blastomeres were examined sequentially during cleavage in selected embryos.

Differential organization and cell-specific intensities of mitochondrial fluorescence from pronuclear to 2-cell stage

Twenty-nine representative pronuclear oocytes (17 2PN, 12 3PN) were examined by SLCM. All oocytes showed centrally located pronuclei with equatorially positioned nucleoli, and varying degrees of cortical clearing or the presence of a perinuclear halo (e.g. asterisks, Figure 1A). When viewed by SLCM, a pronounced accumulation of mitochondrial fluorescence in the peripronuclear cytoplasm was detected in all oocytes (M, Figure 1B). Results obtained from fully compiled images (e.g. Figure 1B) and consecutive SLCM sections (e.g. Figure 1C) demonstrated that mitochondria were concentrated in the perinuclear cytoplasm in an ellipsoidal mass with diminished or virtually no detectable fluorescence in regions of the cortical cytoplasm associated with the cytoplasmic flare or perinuclear halo. For all oocytes, serial optical sections through the perinuclear mass consistently demonstrated that

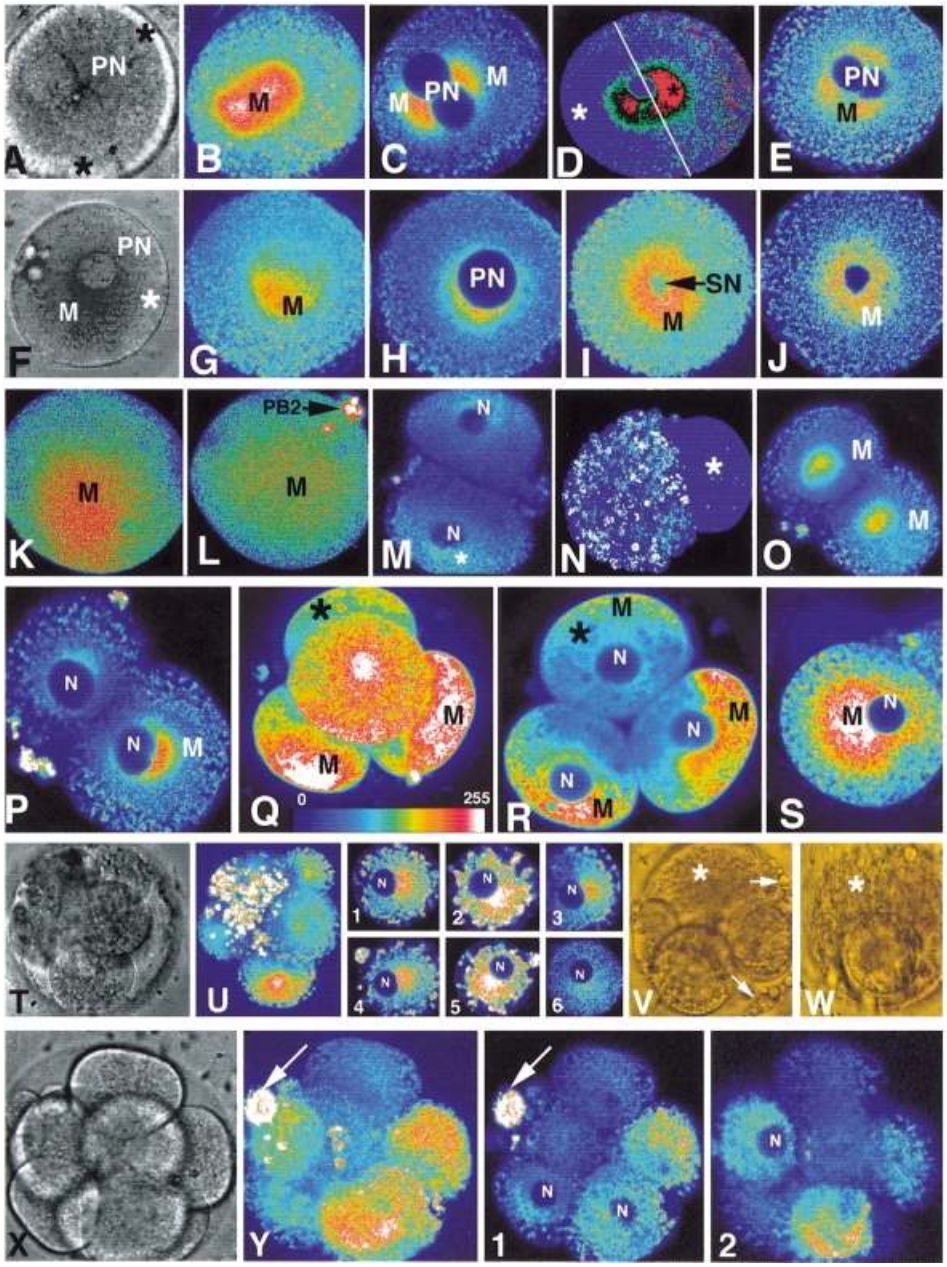

Figure 1. **A**–**H** are light (**A**, **F**) and scanning laser confocal microscopy (SLCM) pseudo-colour images of bipronuclear (**A**–**E**) and unpenetrated, monopronuclear oocytes (**F**–**H**) stained for mitochondria with rhodamine 123 (R123) (**B**, **C**, **E**, **G**–**J**) or noracridine orange (NAO) (**D**) at 16 h after insemination by conventional IVF. **B**, **G** and **H** are fully complied images and **C**-**E** and **H** are 5 μm SLCM sections. The relative intensity of mitochondrial fluorescence is indicated by a colour bar with the lowest intensity at the blue end of the spectrum and the highest in the orange–white region. Oocyte-specific differences in the cytoplasmic and perinuclear (PN) distribution of mitochondria (M) are described in the text. In **D**, the asymmetrical localization of cytoplasmic and perinuclear mitochondria is indicated by a black and white asterisk, respectively; the white line indicates the plane of the first cleavage division observed in time-lapse recordings. **I**–**L** are representative SLCM images of rhodamine (R123)-stained oocytes at the beginning (**I**, **J**, 22 h after insemination) and completion (**K**, 24 h after insemination) of syngamy (SN), and just prior to the first cell division (**L**, PB2 = second polar body). The distribution of mitochondria-specific fluorescence between blastomeres at the 2- (**M**–**P**), 4- (**Q**–**S**), 6- (**T**–**U1**–**6**) and 8-cell stage (**X**, **Y1** and **2**) are presented as SLCM pseudo-colour images after staining with R123 (**M**–**P**, **U**) or NAO (**Q**–**S**, **Y**). **T** and **X** are light microscopic images of the corresponding 6- and 8-cell monospermic embryos. The embryo shown in **N** was examined during the first cell division, and one forming blastomere with significantly reduced R123 fluorescence is indicated by an asterisk. For these representative embryos, mitochondrial organization at the pronuclear and early cleavage stages is discussed in the text. **Q**–**U1**–**6**, and **X**, **Y1** and **2** indicate different intensities of blastomere-specific mitochondrial fluorescence detected in intact (**U**, **Y**) 6- and 8-cell embryos, and individual blastomeres after complete (**U1**–**6**) or partial disaggregation (**Y1**–**2**). **V** and **W** are light microscope images of a 6-cell embryo in which one blastomere observed to have comparatively low mitochondrial fluorescence at the 4-cell stage (similar to blastomere indicated by an asterisk in **R**), began to swell (asterisk, **V**) and burst (asterisk, **W**) during a 16 h culture period. The arrows in Y and Y1 indicate the second polar body. **D** and **N** were published previously in Van Blerkom (2000). N = nucleus.

the highest intensities of mitochondrial fluorescence were localized to the region of pronuclear opposition (Figure 1C-E). For 59% of the monospermic (n = 10/17) and 42% of the dispermic oocytes (5/12) examined in this study, a domain of intense mitochondrial fluorescence was symmetrically distributed around the region of pronuclear opposition (e.g. Figure 1C). For 41% of monospermic oocytes (7/17) and 58% of dispermic oocytes (7/12), the perinuclear domain was asymmetrical with higher mitochondrial density, as indicated by the intensity of fluorescence, largely confined to one 'side' of the opposed pronuclei and the corresponding cytoplasm. This asymmetry was most evident in serial SLCM sections and, for some oocytes, relatively large areas of the cytoplasm appeared virtually devoid of mitochondrial fluorescence (e.g. Figure 1D). Both within and between cohorts, the pattern and symmetry of peripronuclear and cytoplasmic mitochondrial fluorescence was oocyte-specific and unrelated to whether two or three pronuclei were present. During syngamy, high intensities of mitochondrial fluorescence were still associated with the perinuclear cytoplasm (Figure 1I and J), but after syngamy, as shown in Figure 1L, fluorescence in this region became progressively more diffuse. Oocytes in which a significant portion of the cytoplasm was deficient in mitochondria owing to a pronounced asymmetrical distribution during the pronuclear stage (e.g. Figure 1D) retained this condition after syngamy (e.g. Figure 1K).

All unpenetrated monopronuclear oocytes in which a cytoplasmic flare developed (n = 6, asterisk, Figure 1F) showed a perinuclear accumulation of mitochondria (M, Figure 1F) that was asymmetrical when observed by SLCM (Figure 1G and H). In comparison to normally fertilized or dispermic oocytes, monopronuclear oocytes exhibited a perinuclear mitochondrial accumulation of mitochondria in consecutive sections and fully compiled images (e.g. compare Figure 1B and G with 1C and H) that was less pronounced and largely localized to one portion of the single pronucleus. For all unpenetrated monopronuclear oocytes (n = 5) in which no cortical clearing was detected, mitochondria were uniformly distributed with no detectable perinuclear accumulation (comparable to image in Figure 1L). The cleavage potential of unpenetrated monopronuclear oocytes was not determined, as all such oocytes were fixed for tubulin immunofluorescence analysis.

For nine 2-cell embryos that developed from pronuclear oocytes in which the perinuclear accumulation of mitochondria was relatively symmetrical (e.g. Figure 1B and 1C), both blastomeres showed similar intensities and distributions of mitochondrial fluorescence throughout the 2-cell stage (Figure 1O). For eleven 2-cell embryos that developed from pronuclear oocytes with pronounced mitochondrial asymmetry and relatively large regions of cytoplasm devoid of mitochondrial fluorescence, differences in the intensity of R123 and NAO fluorescence between blastomeres were evident in all cases. For example, the representative embryo presented in Figure 1N was examined during the first cleavage division and a very significant reduction in mitochondrial fluorescence is evident in one developing blastomere (asterisk, 10 μm SLCM section). Figure 1D is representative of the type of asymmetrical mitochondrial distribution observed at the pronuclear stage which has been observed to be associated with profound distortions in the pattern of mitochondrial segregation and disproportionate inheritance between blastomeres at the first cell division. The white line in Figure 1D indicates the plane of the first cleavage division observed in time-lapse recordings. Other 2-cell embryos in which the amount of disproportionate mitochondrial segregation was less severe than in the embryos shown in Figure 1D and N, were examined during subsequent cleavage divisions (e.g. Figure 1P).

For 14 embryos observed by SLCM during the first cleavage division, mitochondria segregated in a polarized manner such that the highest intensity of fluorescence was initially detected in the apical cytoplasm of daughter blastomeres (asterisk, Figure 1M). After completion of cytokinesis, a pronounced perinuclear accumulation of mitochondria was evident in all blastomeres (e.g. Figure 1O). Blastomeres with reduced inheritance exhibited pronuclear mitochondrial aggregation, but of lower intensity (e.g. upper blastomere, Figure 1P).

Four- to 16-cell stage

At the 4-cell stage (2PN, derived from: n = 8; 3PN, n = 12), blastomere-specific differences in the relative intensity of mitochondrial fluorescence were clearly evident for 14 embryos that showed similar differences at the 2-cell stage, and which developed from pronuclear oocytes in which mitochondria were asymmetrically distributed. For some embryos (n = 6/20), a reduced amount of mitochondrial fluorescence was observed in one cell (asterisk, Figure 1Q). In order to preclude the possibility that differential mitochondrial fluorescence observed in intact embryos was related to blastomere position during SLCM analysis, these embryos were disaggregated either partially or completely into component blastomeres and rescanned. The representative embryo presented in Figure 1Q-S shows blastomere-specific mitochondrial fluorescence in a fully compiled image of an intact 4-cell embryo from a monospermic fertilization (Figure 1Q) followed by analysis where three blastomeres were left intact (Figure 1R) and the fourth examined in isolation (Figure 1S). The blastomere with reduced mitochondrial fluorescence detected in the intact embryo and after removal of a single blastomere is indicated by an asterisk in Figure 1Q and R, respectively. Sequential fluorescence analysis performed on intact embryos and disaggregated blastomeres at the 4-cell stage (n = 4) showed one or two blastomeres with significantly reduced intensities of NAO fluorescence. All of these embryos had developed from pronuclear oocytes in which a pronounced asymmetry in peripronuclear R123 or NAO fluorescence was evident. Other intact embryos with mitochondrially deficient blastomeres were maintained in culture and examined by SLCM at 24 h intervals (see below).

Shortly after completion of the second cleavage division, the intracellular distribution of mitochondrial fluorescence in each blastomere of the 4-cell embryo was polarized. The highest intensity of R123 or NAO (Figure 1Q and R) was usually detected in the apical cytoplasm and reduced intensity of fluorescence common to those regions of the cytoplasm where blastomeres were in opposition (M, Figure 1R). For some blastomeres, however, the highest concentration of mito-

chondrial fluorescence was not positioned apically, such as shown in Figure 1R. In these instances, differences in the relative position of the mitochondrial aggregate may be related to rotations blastomeres can undergo during early cleavage. In contrast, R123 or NAO fluorescence was uniformly distributed in blastomeres that exhibited low levels of mitochondrial fluorescence (similar to light blue cells in Figure 1Y1). For 4-cell embryos that developed from pronuclear oocytes in which mitochondrial distribution was relatively symmetrical (e.g. Figure 1B), similar intensities of mitochondrial fluorescence were detected between blastomeres (images shown at 8-cell stage, Figure 2A1-8). Monospermic ($n = 6$) and dispermic ($n = 5$) embryos with similar intensities of R123 fluorescence between blastomeres were retained in culture and examined at the 8-16-cell stage for blastomere-specific mitochondrial fluorescence and ATP content.

Differences in the intensity of mitochondrial fluorescence were detected between blastomeres in 6-cell ($n = 4$) and 8-cell ($n = 9$) embryos that developed from the 1-cell stage where an asymmetrically positioned perinuclear mitochondrial aggregate was identified. For these monospermic ($n = 5$) and dispermic ($n = 8$) embryos, the relative intensity of fluorescence was reduced in two or four cells at the 6-cell (Figure 1T and U, U1-6) and 8-cell (Figure 1X, Y, Y1, Y2; Figure 2B1–5) stages respectively. Differential mitochondrial fluorescence between blastomeres was observed by SLCM in intact embryos (Figure 1T and U, Y1 and 2) and confirmed for the same blastomeres after disaggregation (e.g. Figure 1U1–6). Six normal-appearing 8-cell embryos (e.g. Figure 2A) that were observed to have a relatively uniform peripronuclear aggregation of mitochondria at the 1-cell stage (e.g. Figure 1C) were examined in this study. The relative intensity of R123 and NAO fluorescence was largely comparable between blastomeres with relative intensities similar to those shown in Figure 2A1–8. During the early cleavage stages, portions of the cytoplasm devoid of mitochondrial fluorescence were evident (e.g. asterisks, Figure 2A4, 5 and 7, and B2 and 4), but the pronounced apical localization of NAO or R123 fluorescence observed during the 4-cell stage was not as apparent by the 8-cell stage (Figure 2A1–8 and B1–5).

The development of 39 normal-appearing monospermic 4–6-cell embryos (day 3) where half of the blastomeres showed low intensity R123 fluorescence (e.g, Figure 1Y1) was determined during an additional 2 days of culture. Fifty-six per cent (22/39) arrested cleavage at the 8–10-cell stage. Forty-four per cent (17/39) contained between 16 and 21 cells on day 5 and were classified as stage-inappropriate. During additional culture, some blastomeres in which very low R123 or NAO intensities were detected at the 6–8-cell stage arrested division and subsequently lysed. Blastomere lysis was indicated by the elaboration of plasma membrane blebs followed by blastomere swelling and subsequent lysis several hours later. For example, Figure 1V and W are time-lapse images of a 6-cell embryo which appeared normal at 50 h post-insemination (day 2.5), but where the relative intensity of R123 fluorescence in one blastomere was clearly reduced at the 4-cell stage when compared to other cells in the embryo (similar to Figure 2B1). At 58 h, small plasma membrane blebs were observed on cell surface of this blastomere, some of which eventually detached and were detectable as discrete entities in the perivitelline space (arrows, Figure 1V). At 65 h, this blastomere appeared to swell (asterisk, Figure 1V) and its increased size was accompanied by a reduction in cytoplasmic density. Fourteen hours after blebs were first detected (72 h), and 6 h after swelling was initially observed, this blastomere abruptly burst, leaving behind a cytoplasmic matrix (asterisk, Figure 1W) enclosed by remnants of the plasma membrane and small membraneous ghosts in the perivitelline space. Cell division continued in this representative embryo and 18 mononucleated blastomeres were counted on day 5. The embryo shown in Figure 2B1–5 is also representative of an apparently normal appearing monospermic 8-cell embryo that developed from a 'high competence' pronuclear embryo with asymmetrically localized mitochondria. For embryos of this type, where several blastomeres showed low R123 (or NAO) intensity, development beyond the 8–10-cell stage was not observed after 2.5 additional days, at which time culture was terminated. To date, the developmental capacity of 16 monospermic embryos with comparable levels of blastomere R123 fluorescence (similar to Figure 2A1–8) at the 8-cell stage has been examined during 6 days of culture, as described previously (Van Blerkom, 1993). Eleven embryos (68%) developed into blastocysts, two (13%) showed signs of cavitation, and three were compacted morulae (19%). If confirmed, this preliminary finding suggests that mitochondrial inheritance among blastomeres may be one factor that influences the ability of the human embryo to develop progressively.

For normally developing, stage-appropriate embryos, comparable intensities of R123 fluorescence that were previously observed between blastomeres at the 4- and 8-cell stages were no longer apparent at 12–16-cell stage. While only four monospermic 12–16-cell embryos of this type were examined, R123 fluorescence was clearly detectable in all mono- (e.g. Figure 2C2, 4 and 11) and binucleated (Figure 2C3) blastomeres and differed in intensity between blastomeres, as shown for 12 cells of one such embryo in Figure 2C1–12. Blastomeres from these embryos were used for ATP determination (see below). However, the position of individual cells in the intact embryos (inside or outside) was not correlated with specific blastomeres after disaggregation. The intensity of R123 fluorescence was examined in 13 binucleated blastomeres (e.g. Figure 2C3) obtained from 13 normal appearing 8–12-cell monospermic embryos. The relative intensities of mitochondrial fluorescence in these cells were largely comparable to those observed in mononucleated blastomeres in the same embryo (e.g. compare Figure 2C3 and 4).

Quantitative determinations of blastomere-specific ATP content in normal and slow developing 8–10-cell embryos

Whether the net ATP content of an individual blastomere and apparent intensities of mitochondrial R123 fluorescence were related was determined by measuring blastomere-specific net ATP content after SLCM analysis. The values presented in Table I are representative results from two classes of cleavage stage embryos that were available for analysis: (i) intact, stage-appropriate embryos (8–10 cells on day 3, $n = 9$) with

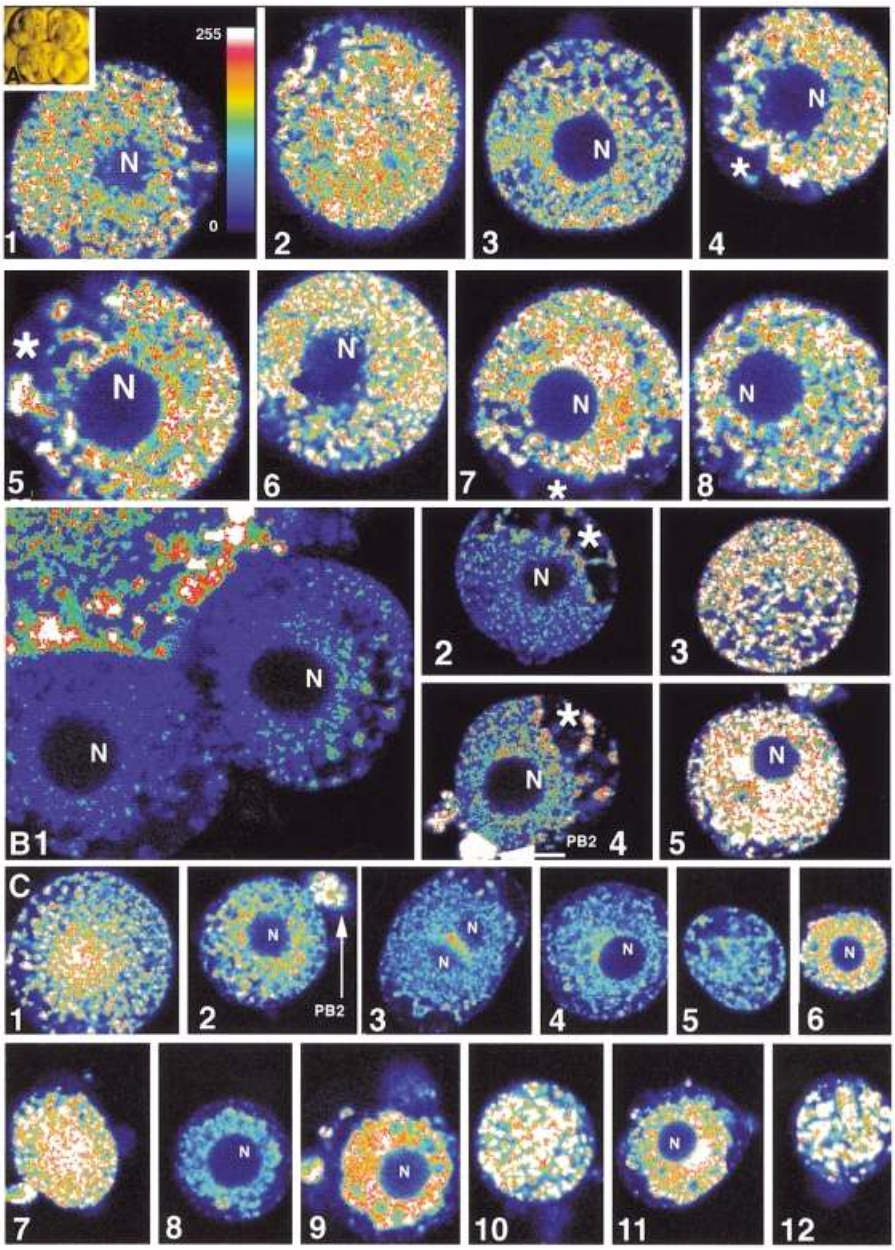

Figure 2. Representative blastomere-specific rhodamine (R123) fluorescence shown in scanning laser confocal microscopy (SLCM) pseudo-colour images (8 μm sections, **A1**–**8**) of a normal monospermic (**A**) 8-cell embryo that developed from a pronuclear embryo with symmetrical peripronuclear mitochondrial organization. Typical ATP contents for embryos of this type are presented in Table I. **B1**–**5** (8 μm sections) shows seven blastomeres of an 8-cell embryo with different intensities of R123 fluorescence typical of cleavage stage embryo that developed from a pronuclear embryo with asymmetric mitochondrial distribution. Typical ATP contents for embryos of this type are presented in Table I. **C1**–**12** (5 μm sections) are representative blastomere-specific R123 fluorescence in an apparently normal monospermic 12-cell embryo that developed from a pronuclear embryo with symmetrical peripronuclear mitochondrial organization. A single binucleated blastomere is shown in **C3**. The asterisks indicate areas of cytoplasm devoid of detectable mitochondrial fluorescence (see text for details). N = nucleus; PB2 = 2nd polar body.

comparable intensities of mitochondrial fluorescence between blastomeres determined by sequential analysis from the 2-cell stage (e.g. Figure 2A1-8), and (ii) intact (unfragmented) monospermic embryos that were classified as 'slow developing' and stage inappropriate (e.g. 8-cell on day 3.5, Figure 2B1–5, n = 9; 10–12-cell on day 4.5, n = 11). Slow-developing embryos were derived from pronuclear oocytes with asymmetric mitochondrial distribution and different intensities of R123 fluorescence were detected between blastomeres at the 2-cell stage.

In Table I, representative ATP contents are expressed in fmoles for total ATP/blastomere and as amol/μm^3 after adjustment for blastomere volume. For example, 8–10-cell embryos (n = 9) with comparable levels of R123 fluorescence had comparable ATP contents after normalization of volumes between blastomeres (amol/μm^3). For stage-inappropriate

Table I. Representative distribution of rhodamine 123 fluorescence and ATP content between blastomeres of cleavage stage human embryos with normal and slow rates of development

Stage/blastomere	Apparent rate of development			
	Normal		Slow	
	Total ATP (fmol)	ATP/μm^3 (amol)	Total ATP (fmol)	ATP/μm^3 (amol)
8-Cell				
1	402	9.2	397	10.4
2	361	8.6	372	9.9
3	290	8.4	188	8.0
4	230	8.3	199	6.5
5	246	8.3	235	5.4
6	226	8.2	388	3.6
7	402	7.6	119	1.6
8	216	7.2	126	1.1
10-Cell				
1	272	10.4	693	10.6
2	221	8.6	351	9.9
3	464	8.5	481	8.4
4	226	8.4	261	8.3
5	419	8.0	179	8.7
6	385	7.9	207	6.3
7	264	7.7	192	3.1
8	307	7.6	320	2.8
9	444	7.2	119	2.7
10	570	7.2	133	1.3

ATP contents are expressed in fmoles for total ATP/blastomere and as amol/μm^3 after adjustment for blastomere volume.

embryos where R123 fluorescence between blastomeres was clearly different (e.g. Figure 2B1-5), the lowest and highest ATP contents were measured in blastomeres with correspondingly low (e.g. Figure 2B1) and high R123 fluorescence (e.g. Figure 2B3). The same findings were obtained after adjusting volume calculations of cytoplasmic fluorescence for differences in nuclear/cytoplasmic ratios. For example, embryos classified as stage appropriate at 72 h after insemination, the ATP amol/μm^3 was comparable between blastomeres with concentrations between 7.0 and 9.0 amol/μm^3/blastomere detected. For eight 8-cell embryos whose cleavage rate was classified as 'slow', blastomere-specific ATP contents ranged from 1.1 to 10.4 amol/μm^3 (e.g. Figure 2B1–5). In preliminary studies of 12–16-cell embryos classified as normally progressing ($n = 4$) or slow-dividing ($n = 10$) on days 3.75 and 4.75 respectively, the distribution of ATP contents between blastomeres showed differences comparable to intensities of R123 fluorescence and ATP content detected in these types of embryos at the 8-cell stage. For normal 12-cell embryos (e.g. Figure 2C1–12), ATP contents/blastomere ranged from approximately 7.0 to 11 amol/μm^3. For embryos classified as stage inappropriate on days 4 and 5, the ATP content of about half of the blastomeres was $\leqslant$3.0 amol/μm^3, with concentrations measured in other blastomeres comparable to or higher than those determined for embryos classified as stage-appropriate. In five slow developing embryos, blastomeres with very high intensity R123 fluorescence had ATP contents between 14–17 amol/μm^3. The inter-assay variance with split samples from individual blastomeres was $\pm$1%. The ATP contents of binucleated blastomeres were comparable to their mononucleated counterparts.

Microtubule organization in pronuclear and early cleavage stage embryos

All 10 unpenetrated monopronuclear oocytes examined in this study that exhibited an asymmetrical perinuclear aggregation of mitochondria (e.g. Figure 1G, H) and a cytoplasmic flare (asterisk, Figure 1F) showed a corresponding asymmetry in the distribution of microtubular arrays that extended into the cytoplasm from the vicinity of the nuclear membrane (Figure 3A). Cytoplasmic regions with reduced intensities of mitochondrial fluorescence were largely devoid of microtubules (asterisk, Figure 3A). For these activated oocytes, SLCM analysis showed several intense foci of tubulin fluorescence associated with the nuclear membrane with arrays of microtubules emanating from these structures. Serial SLCM sections through the nuclear region indicated that these foci were not uniformly distributed but rather clustered to one region of the nuclear membrane (arrows, Figure 3B). For all six unpenetrated monopronuclear oocytes in which no cytoplasmic flare was evident, a uniform cytoplasmic distribution of mitochondrial fluorescence was observed. The cytoplasm was devoid of detectable microtubules, and no perinuclear foci of tubulin immunofluorescence was detected (Figure 3C).

All normally fertilized ($n = 11$) and dispermic (tripronuclear, $n = 13$) oocytes classified as high competence contained a well-developed mictotubular network (Figure 3D-F) with arrays of microtubules radiating from the nuclear region. For most oocytes examined in serial SLCM sections ($n = 15/24$), microtubule immunofluorescence was detected throughout the cytoplasm with a comparative increase in network density detectable in one portion of the cytoplasm (e.g. asterisk, Figure 3D). Regions of the cleared cortical cytoplasm were largely

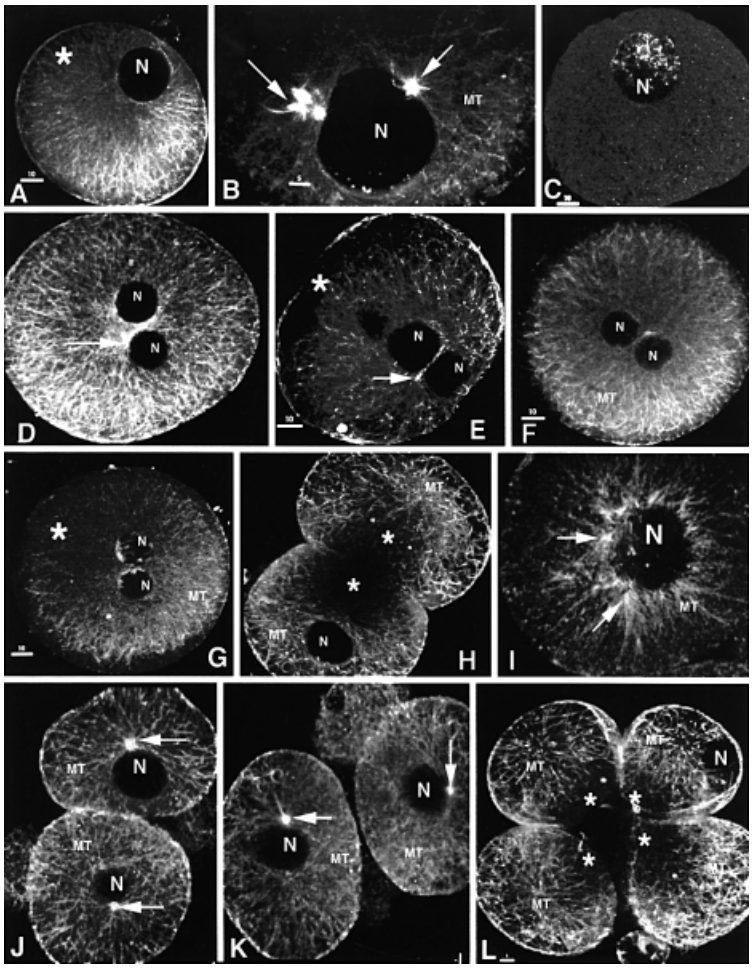

Figure 3. Sections (5 μm thick) scanning laser confocal microscopy (SLCM) of anti-tubulin immunofluorescence in unpenetrated mono- (**A**–**C**) and monospermic bipronuclear human oocytes (**D**–**G**) and 2- (**H**, **I**) 4- (**J**, **K**) and 8-cell stage monospermic embryos (**L**). These samples were selected for analysis according to patterns of mitochondrial distribution observed with R123 or NAO in the living state. Perinuclear foci of intense anti-tubulin fluorescence are indicated by arrows and regions devoid of detectable fluorescence are indicated by an asterisk. **C** and **G** were also stained for nuclear (N) DNA. MT = microtubules. See text for details.

devoid of microtubular immunofluorescence (asterisk, Figure 3E). However, for some pronuclear oocytes (n = 9/24) a pronounced asymmetry in the distribution of microtubular arrays was evident (e.g. asterisk, Figure 3G). For these monospermic and dispermic oocytes, relatively large regions of the cytoplasm contained a scant population of microtubules.

For all 24 high competence pronuclear oocytes examined, increased intensities of mitochondrial R123 and NAO fluorescence were associated with regions of the cytoplasm containing the highest apparent density of microtubules. For example, the region indicated by an asterisk in Figure 3G was virtually devoid of mitochondrial fluorescence similar to the image shown in Figure 1D. The relative symmetry of peripronuclear mitochondrial fluorescence was associated with the pattern and density of microtubular arrays extending into the cytoplasm from the nuclear region, including those originating from distinct perinuclear foci (e.g. arrows, Figure 3D and E).

During formation of the 2-cell embryo (n = 6), the highest density of microtubules was located in the apical cytoplasm with virtually no detectable microtubules in basal regions where segregation of the cytoplasm into daughter blastomeres was taking place (asterisks, Figure 3H). This arrangement of microtubules was correlated with the distribution of mitochondrial fluorescence at this stage (e.g. Figure 1M). The varying patterns and intensities of perinuclear mitochondrial fluorescence observed during the 2-cell stage (Figure 1O and P) correspond to differences in the organization and density of perinuclear microtubules that appear to be cell cycle-related. For example, perinuclear mitochondrial fluorescence that was relatively intense and symmetrically distributed (e.g. Figure 1O) occurred in blastomeres where arrays of nuclear membrane-associated microtubules radiated into the adjacent cytoplasm in a largely radial fashion during the early 2-cell stage (e.g. Figure 3I).

All blastomeres of 4-cell (n = 6) and 8-cell embryos (n = 5) derived from pronuclear oocytes with symmetrically distributed mitochondria exhibited similar patterns of microtubular distribution. Typically, the density of the microtubular network in these embryos was reduced in one portion of each blastomere (MT, Figure 3J and K). Each nucleus was associated with at least one focus of intense tubulin fluorescence (arrows, Figure 3J and K). For each blastomere at the 4-cell stage, the region of cytoplasm associated with the highest intensities of mitochondrial fluorescence (e.g. Figure 1R and S) occurred in

regions containing the highest density of microtubules as observed in serial SLCM sections and fully complied images. At the 8-cell stage for both monospermic ($n = 3$) and dispermic embryos ($n = 8$), microtubules were found throughout the cytoplasm (Figure 3L). However, microtubules were often deficient in basal regions of the cytoplasm where blastomeres were opposed (asterisks, Figure 3L). For these blastomeres, mitochondrial fluorescence was also diminished or absent in these regions (e.g. Figure 2A4 and 5, and B2 and 4). For 4- ($n = 4$) and 8-cell embryos ($n = 5$) that developed from pronuclear oocytes with highly asymmetric mitochondrial distributions (e.g. Figure 3L), the perinuclear and cytoplasmic distribution of microtubules in blastomeres with relatively normal levels of R123 fluorescence was comparable to organizations detected in cleavage stage embryos that developed from pronuclear oocytes with symmetrically distributed mitochondria. In contrast, for blastomeres with very low intensity R123 or NAO fluorescence (e.g. asterisk Figures 1N and 2B1), the cytoplasm was devoid of microtubules detectable by SLCM (similar in appearance to Figure 3C).

Discussion

The ability to predict developmental competence within cohorts of cultured embryos and select for transfer only those with the highest potential to implant has been one of the foremost challenges in clinical IVF. Reliance on morphological criteria such as rates of cell division, uniformity of blastomeres, and estimates of the degree of fragmentation have been the primary determinants of embryo selection for cleavage stage embryos (day 2 or 3). However, developmental arrest of intact embryos *in vitro*, and implantation failure or a singleton implantation after transfer of multiple embryos, are difficult to explain when all exhibit equivalent and normal morphology during cleavage. Recent studies of outcome after IVF suggest that the following characteristics of nuclear and cytoplasmic organization at the 1-cell stage may be highly indicative of competence: (i) an equatorial alignment of nucleoli at the region of pronuclear opposition (Scott and Smith, 1998; Tesarik and Greco, 1999), (ii) a focal change in the texture of the cortical cytoplasm (cytoplasmic flare; Payne *et al*., 1997) which progresses to involve the entire cytocortex (pronuclear halo; Scott and Smith, 1998), and (iii) pronuclear orientation with respect to the polar bodies (Garello *et al*., 1999). The absence of a specific pattern of nucleolar alignment and the failure of a cytoplasmic flare or perinuclear halo to develop have been correlated with poor competence. In the same respect, different pronuclear orientations have been correlated with the normality of cleavage, and significant deviations from specific alignments were reported to predispose the affected embryos to common cleavage anomalies such as fragmentation and unequal cell divisions, two significant phenotypes that have been associated with early developmental arrest and implantation failure (Garello *et al*., 1999). Pronuclear orientation and cortical clearing may be related epigenetic factors that influence competence by determining how cytoplasmic components, including proteins and nascent transcripts of putative regulatory genes are distributed, or the pattern by which the plane of the first cleavage division bisects the oocyte (Edwards and Beard, 1997; Garello *et al*., 1999).

Here, evidence is provided that mitochondrial distribution at the pronuclear stage may be another epigenetic factor related to the organization of the 1-cell embryo that is developmentally relevant with respect to embryo competence. The recognition that mitochondria have a fundamental role in the normality and success of early human development has emerged recently as one possible explanation for early developmental failure in general and the progressively higher frequencies of failure observed in women of advanced reproductive age in particular (Jansen and de Boer, 1998). One current view of mitochondrial function is that reduced meiotic competence and fertilizability for the oocyte (Barritt *et al*., 1999; Perez *et al*., 2000) and developmental failure in the preimplantation embryo could result from pre-existing oocyte mitochondrial DNA (mtDNA) defects, or from an age-related accumulation of mtDNA mutations (Keefe *et al*., 1995). Presumably, mtDNA defects that reduce oxidative phosphorylation capacity could have adverse developmental consequences if accompanied by diminished ATP. An inability to regulate or mobilize intracellular calcium could be a functional defect in genetically altered mitochondria which may affect cell cycle regulation in the early embryo (Sousa *et al*., 1997). However, the extent (if any) to which specific human oocyte mtDNA defects are proximate causes of early reproductive failure or are related to specific aetiologies of infertility has yet to be determined unambiguously (see below, and Brenner *et al*., 1998).

The relative contribution of mitochondrial oxidative phosphorylation to ATP production during the preimplantation stages has been examined in several mammals, including mice, rats, cows, and humans (Magnusson *et al*., 1986; Hardy *et al*., 1989; Gott *et al*., 1990, Brison and Leese, 1994; Houghton *et al*., 1996; Thompson *et al*., 1996, 2000), and the findings indicate that ATP generation during pre-compaction stages is largely dependent upon oxidative phosphorylation, with a shift to glycolysis occurring during cavitation and the blastocyst stages (see review by Van Blerkom *et al*., 1998). In support of this notion is the birth of mice that developed from embryos exposed to inhibitors of mitochondrial protein (31.2 μg/ml, chloramphenicol) and RNA synthesis (0.1 μg/ml, ethidium bromide) during the preimplantation stages (Piko and Chase, 1973). Because these biosynthetic activities are normally activated between 8- and 16-cell stages in the mouse (Piko and Chase, 1973), pre-existing (oocyte) mitochondrial proteins and transcripts are likely utilized prior to cavitation to generate ATP. At higher concentrations, Piko and Chase (1973) reported developmental delay or arrest, suggesting that mitochondrial sensitivity to these inhibitors may exist in early cleavage stage embryos. Van Blerkom *et al*. (1995b) showed that mouse oocytes exposed to uncouplers of mitochondrial oxidative phosphorylation matured *in vitro* with net ATP contents significantly below values present in untreated controls. While treated oocytes were fertilizable, development was severely compromised with most arresting during cleavage. Other species, such as the bovine, appear to be less dependent upon mitochondrially generated ATP during cleavage, at least *in vitro*, as indicated by the ability of early embryos to up-

regulate glycolysis in the presence of inhibitors of oxidative phosphorylation (Brison and Leese, 1994; Thompson *et al*., 1996, 2000).

For the human, mitochondrial oxidative phosphorylation may be the primary mechanism of ATP generation in the oocyte, newly fertilized oocyte and pre-compaction cleavage stage embryo. In this respect, it has been suggested that mitochondrial 'transfusion' into MII oocytes by cytoplasmic donation (Cohen *et al*., 1998) or by direct injection of these organelles (Van Blerkom *et al*., 1998) may be one factor associated with an apparent improvement in the normality of development during early cleavage and outcome after embryo transfer in some women who previously failed to conceive (with their untreated gametes). Decreased mitochondrial inheritance in early blastomeres owing to disproportionate segregation may account for the reduced ATP content detected in cells with diminished or poor R123 or NAO fluorescence. The extent to which mitochondrially deficient blastomeres may be able to compensate for reduced oxidative phosphorylation capacity by up-regulating glycolytic activity, as recently reported for cultured bovine oocytes (Krisher and Bavister, 1999) and embryos (Thompson *et al*., 2000), is unclear. However, the arrest of cell division and eventual cell death for affected blastomeres suggests that diminished ATP generating capacity can have adverse developmental, if not lethal consequences.

The apparent reliance on oxidative phosphorylation in maturing oocytes and early embryos may explain why, in some species, mitochondria undergo redistribution at these stages. During meiotic maturation of the mouse oocyte, mitochondria are translocated to the nuclear region during germinal vesicle break down and MI spindle formation (Van Blerkom and Runner, 1984; Tokura *et al*., 1993) along arrays of microtubules emanating from perinuclear microtubule organizing centres (Van Blerkom, 1991). In pronuclear hamster oocytes and early cleavage stage embryos, stage-specific mitochondrial redistributions include a pronounced translocation to the nuclear region, which is apparently mediated by cytoarchitectural elements (Barnett *et al*., 1996). Perturbations from normal patterns of mitochondrial translocation and distribution during oocyte maturation in the mouse (Van Blerkom, 1991) and early cleavage in the hamster (Barnett *et al*., 1997) have been shown to have lethal consequences. It seems that the maturing oocytes and newly fertilized oocytes of several species have developed a common strategy to adjust mitochondrial density to different intracellular regions where locally high concentrations of ATP (Van Blerkom and Runner, 1984) or mobilized calcium (Sousa *et al*., 1997) may be required at different stages of development. The possibility that a similar pattern of mitochondrial redistribution occurs during early human development and may be of developmental significance is discussed below.

Disproportionate mitochondrial inheritance occurs during cleavage

Here, fluorescent probe analysis by SLCM demonstrates that development in newly fertilized oocytes exhibiting morphodynamic characteristics suggestive of competence is associated with a pronounced ellipsoidal accumulation of mitochondria around the opposed pronuclei. Peripronuclear aggregation is accompanied by the depletion of mitochondria from the cortical cytoplasm where a cytoplasmic flare is detectable or circumferential clearing of the cytocortex produces a pronuclear halo. However, the results also demonstrate that significant differences in peripronuclear mitochondrial organization occur between oocytes in the same and different cohorts, which range from relatively symmetrical to grossly asymmetrical. When pronuclear oocytes with a pronounced asymmetrical distribution of mitochondria were examined during syngamy, mitochondrial distribution remained asymmetrical and when re-examined after the first cell division mitochondrial inheritance, as indicated by the intensity of R123 or NAO, fluorescence differed between daughter blastomeres. If cleavage progressed to the 4–6-cell stage, one or two blastomeres showed intensities of mitochondrial fluorescence that were reduced considerably when compared to other blastomeres in the same embryo. Analysis of ATP content demonstrated comparatively low amounts in blastomeres with reduced mitochondrial fluorescence. As reported elsewhere (Van Blerkom, 2000), blastomeres that are profoundly deficient in mitochondrial fluorescence at the first or second cleavage division remain undivided and often die during subsequent culture.

The current protocol does not permit transfer of embryos exposed to fluorescent probes, and, consequently, whether outcome is related to specific patterns of mitochondrial inheritance observed during early cleavage is unknown. However, the occurrence of a single blastomere with poor mitochondrial fluorescence and reduced ATP content at 4–6-cell stage does not necessarily indicate a premorbid or developmentally adverse condition because cell division continued in other blastomeres. In contrast, competence was impaired significantly in embryos derived from pronuclear oocytes where pronounced mitochondrial asymmetry was associated with half of the blastomeres in 6- and 8-cell stage embryos exhibiting poor R123 or NAO fluorescence. In these instances, cell division arrested for the affected blastomeres, and, for the embryo, development either arrested or progressed slowly, with cell numbers clearly inappropriate for days 3–5 of culture. It is suggested that the number of blastomeres affected by disproportionate mitochondrial inheritance may be a proximal determinant of developmental competence.

Blastomere-specific differences in R123 intensity were detected in all 12–16-cell embryos that were stage appropriate with respect to cell number on days 3 and 4 of culture. Because none of these embryos showed pronounced asymmetry in mitochondrial distribution at the pronuclear stage, it is unlikely that these differences are related to aberrant segregation patterns at the first cell division. However, neither the ATP content nor the relative intensity of R123 fluorescence detected in these blastomeres occurred at the reduced amounts observed in arrested blastomeres. The variability in R123 intensity and ATP content detected in presumably normal 12–16 cell embryos may indicate stage-specific differences in amounts of ATP generation between blastomeres, perhaps reflecting differential activation of glycolysis, or possibly cell position, which may

influence relative substrate availability, especially for those cells in the interior of the embryo.

The human mitochondrial respiratory chain involves 83 polypeptides, 70 of which are encoded by nuclear genes and 13 by mtDNA (Leonard and Schapira, 2000). Normal mitochondrial function and replication are dependent upon the interaction of nuclear and mitochondrial genes, and abnormalities of either genome can result in mitochondrial disease (Larsson and Clayton, 1995; Chinnery and Turnbull, 1999). An essential role for mitochondrially generated ATP in early human development would seem to be negated by the birth of infants with mitochondrial diseases (OXPHOS diseases) inherited from the oocyte and which effect the efficiency of oxidative phosphorylation. While some of these diseases are lethal during gestation or shortly after birth, others result in debilitating or fatal pathophysiologies associated with progressive tissue and organ degeneration later in life (DiMauro, 1998). Although it is unknown which, if any, mitochondrial diseases are lethal prior to implantation, the occurrence of individuals with OXPHOS disorders would tend to suggest that early cleavage may not have an absolute requirement for this mode of ATP generation. However, it is possible that if embryo mitochondrial respiration occurs at a reduced level, a threshold may exist that is consistent with early embryogenesis as long as mitochondrial segregation between blastomeres was largely equivalent. It is unknown whether rates of cell division, blastocyst expansion and hatching in affected embryos may be slower than normal or delayed, as has been shown for mouse embryos cultured in the presence of inhibitors of mitochondrial transcription and translation (Piko and Chase, 1973). In this respect, the pathogenic effects of OXPHOS defects, whether involving proteins encoded by nuclear or mtDNA, may not compromise preimplantation development, but will have downstream consequences associated with cell-type or organ-specific dysfunction that are related to tissue-specific requirements for mitochondrially derived ATP (Schon and Grossman, 1998; Leonard and Schapira, 2000). For normal cleavage stage embryos, it is proposed that blastomere arrest or demise occurs when disproportionate mitochondrial inheritance is accompanied by a diminished capacity to generate ATP at threshold values. In these instances, the response of the affected blastomere(s) may be similar to that experienced by specific tissues in individuals with OXPHOS diseases that perturb normal function or are ultimately fatal in certain cell types (e.g. nerve, muscle; Hammans, 1994). This notion is further supported by previous findings that correlated implantation potential and embryo ATP content (Van Blerkom *et al*., 1995b).

The presence of a non-dividing binucleated blastomere(s) appears to be a common feature of mid–late cleavage stage human embryos that does not seem to adversely effect competence (Tesarik, 1994). In this study, the possibility that multinucleation occurs in blastomeres where a reduced ATP environment resulted from mitochondrial malsegregation during previous divisions was examined. The rationale for this analysis was the assumption that a threshold amount of ATP related to the mitochondrial content of a particular blastomere may be permissive for DNA replication and nuclear membrane assembly but not for cytokinesis. Here, relative levels of R123 fluorescence and ATP content were determined for 13 binucleated blastomeres in thirteen 12–16-cell embryos. The findings demonstrated that ATP contents and fluorescent intensities in binucleated blastomeres were largely comparable to amounts detected in mononucleated cells from the same and from different embryos. It appears that diminished ATP production is an unlikely cause of binucleation. However, whether other blastomere-specific chromosomal defects such as aneuploidy and chaotic mosaicisms may be related to reduced ATP generation associated with disproportionate mitochondrial segregation remains to be determined.

Cytoarchitecture and mitochondrial distribution

Owing to the reported relationship between cytoplasmic microtubular organization and stage-specific mitochondrial distributions in rodent oocytes and cleavage stage embryos, studies were performed to examine whether a similar dynamic process may be involved in the generation of disproportionate mitochondrial inheritance during early cleavage in the human. Unpenetrated, monopronuclear oocytes were particularly informative because development of microtubular configurations reflects inherent oocyte capacities, i.e. those which arise in the absence of a sperm centrosome contribution. Under the light microscope, a cytoplasmic flare or cortical clearing was evident in some monopronuclear examined during the first 24 h after insemination, while others showed no change in cytoplasmic organization. The distribution of mitochondria was associated with the presence or absence of cortical clearing and was asymmetric with respect to the maternal pronucleus in oocytes with focal cortical clearing, or uniformly distributed throughout the cytoplasm in oocytes in which cortical cytoplasmic organization remained unchanged. In oocytes that showed cortical clearing, asymmetrical arrays of microtubules extended into the cytoplasm from the nuclear membrane. In these oocytes, serial SLCM sections demonstrated intense foci of tubulin fluorescence asymmetrically localized on the nuclear membrane from which arrays of microtubules emanated. In contrast, unpenetrated monopronuclear oocytes that showed uniform mitochondrial distributions were virtually devoid of detectable microtubules and, in this respect, resembled the cytoplasm of the metaphase II human oocyte (Van Blerkom *et al*., 1995a). These findings suggest that stage-specific changes in cytoplasmic organization that affect the formation of microtubular arrays and the distribution of mitochondria represent an inherent developmental ability expressed in human oocytes that activate spontaneously or as a consequence of sperm penetration. The absence of cytoplasmic arrays of microtubules and no detectable perinuclear mitochondrial translocation in monopronuclear oocytes without cortical clearing could indicate that the ability to promote microtubule polymerization, but not pronuclear formation, may have failed to develop during meiotic maturation.

Pronuclear oocytes with high competence characteristics showed differences in the distribution of mitochondria that correlated with the organization of microtubules extending from the vicinity of the pronuclear membranes. An asymmetrical distribution of mitochondria was associated with a dense

microtubular network localized to one portion of the oocyte with relatively large regions of cytoplasm devoid of either fluorescent signal. The extent to which arrays of microtubules that develop from the sperm centrosome contribute to perinuclear mitochondrial aggregation is unknown. However, previous studies suggest that it may be significant (Ash *et al*., 1995; Van Blerkom and Davis, 1995; Van Blerkom *et al*., 1995a) and in this study could account for the more pronounced aggregation of mitochondria observed in fertilized oocytes, as opposed to unpenetrated monopronuclear oocytes. Regions of the cleared cortical cytoplasm involved in the cytoplasmic flare or perinuclear halo were devoid of detectable mitochondrial fluorescence and tubulin immunofluorescence. In the developing cleavage stage embryo, regions deficient in mitochondrial fluorescence were also deficient in microtubules, and a transient perinuclear accumulation of mitochondria detected in early cleavage-stage blastomeres was associated with the presence of radial arrays of nuclear membrane-associated microtubules. These results indicate that dynamic and stage-specific changes in mitochondrial distributions during early human development are directed or influenced by intrinsic patterns of microtubular distribution and orientation.

Mitochondrial distribution and competence

It has previously been reported that the extensive network of cytoplasmic microtubules detected during the pronuclear stages disassembles during syngamy with microtubular arrays confined to the nascent mitotic spindle (Van Blerkom *et al*., 1995a). This change in cytoplasmic microtubule organization together with cytoplasmic turbulence (Edwards and Beard, 1997) may account for the progressive redistribution of perinuclear mitochondria detected between syngamy and the first cleavage division. There may be no adverse developmental consequences if the meridional plane of the first cell division partitions a mitochondrial aggregate where peripronuclear asymmetry was not pronounced. Where, mitochondrial aggregation was largely asymmetrical and this asymmetry persisted during syngamy, an epigenetic basis for the observed non-equivalence of mitochondrial distribution at the first cell division may occur if the meridional plane of cleavage bisects the syngamic oocyte in the normal fashion (Edwards and Beard, 1997). For the affected blastomere and its progeny, if any, a significantly reduced capacity to generate ATP by oxidative phosphorylation may be one developmental consequence of disproportionate mitochondrial segregation at the first cell division, and, with continued culture, arrested cell division and death may be the outcome. The absence of cytoplasmic arrays of microtubules in blastomeres with poor mitochondrial inheritance is consistent with compromised cell function. For the embryo, the results of the current study suggest that arrested development occurs when disproportionate mitochondrial inheritance during early cleavage results in about half of the blastomeres exhibiting reduced mitochondrial fluorescence. The extent to which differences in competence are related to specific patterns of mitochondrial inheritance and attendant metabolic capacities will need to be determined clinically with mitochondrial distributions assessed non-invasively. One method that may be applicable to the human is confocal microscopy at the 1047 nm wavelength, which has been recently used to study stage-specific mitochondrial distributions during the development of the preimplantation hamster embryo (Squirrell *et al*., 1999).

In the present study, only those intact embryos that developed from pronuclear oocytes with an equatorial nucleolar alignment and a cytoplasmic flare or perinuclear halo were examined. However, even when these apparent characteristics of competence were present, during cleavage, differences in mitochondrial inheritance were observed between blastomeres; it is suggested that depending upon degree, they are significant with respect to the ability of the affected embryo to develop progressively. Currently, studies are being performed to investigate whether differences in the extent/pattern of cortical clearing (focal or circumferential) are related to cytoplasmic and peripronuclear mitochondrial distributions at the 1-cell stage that could influence mitochondrial segregation during the first cleavage division. Whether the absence of a cytoplasmic flare or perinuclear halo, which has been correlated with poor implantation potential (Scott and Smith, 1998), is associated with patterns of mitochondrial distribution and microtubular configurations that are different from those observed in 'high competence' pronuclear oocytes remains to be determined. However, an association between mitochondrial organization and competence, especially one that can be determined non-invasively during the earliest stages of development, would go a long way in establishing an epigenetic basis for unanticipated developmental arrest *in vitro* and differences in outcome observed with human embryos that appear normal at transfer.

Acknowledgements

We thank Deborah Campbell and Sandra Hahn for their clinical contributions.

References

Ash, R., Simerly, C., Ord, T. *et al*. (1995) The stages at which human fertilization arrests: microtubule and chromosome configurations in inseminated oocytes which failed to complete fertilization and development in humans. *Mol. Hum. Reprod*., **1**, see *Hum. Reprod*., **10**, 1897-1906.

Barnett, D., J., Kimura, J. and Bavister, B. (1996) Translocation of active mitochondria during hamster preimplantation embryo development studied by confocal scanning microscopy. *Dev. Dyn*., **205**, 64–72.

Barnett, D., Clayton, M., Kimura, J. and Bavister, B. (1997) Glucose and phosphate toxicity in hamster preimplantation embryos involves disruption of cellular organization, including the distribution of active mitochondria. *Mol. Reprod. Dev.*, **48**, 227–237.

Barritt, J., Brenner, C., Cohen, J. and Matt, D. (1999) Mitochondrial DNA rearrangements in human oocytes and embryos. *Mol. Hum. Reprod*., **5**, 927–933.

Brenner, C., Wolney, Y., Barritt, J. *et al*. (1998) Mitochondrial DNA deletion in human oocytes and embryos. *Mol. Hum. Reprod*., **4**, 887–892.

Brison, D. and Leese, H. (1994) Blastocoel cavity formation by preimplantation rat embryos in the presence of cyanide and other inhibitors of oxidative phosphorylation. *J. Reprod. Fertil*., **101**, 305–309.

Chinnery, P. and Turnbull, D. (1999) Mitochondrial DNA and disease. *Lancet*, **354**, si17-21.

Cohen, J., Scott, R., Alikani, M. *et al*. (1998) Ooplasmic transfer in mature human oocytes. *Mol. Hum. Reprod.*, **4**, 269–280.

Coulam, C., Goodman, C. and Rinehart, J. (1999) Color Doppler indices of follicular blood flow as predictors of pregnancy after in-vitro fertilization and embryo transfer. *Hum. Reprod*., **14**, 1979–1982.

DiMauro, S. (1998) Mitochondrial diseases: clinical considerations. *BioFactors*, **7**, 277–285.

Edwards, R.G., and Beard, H.K. (1997) Oocyte polarity and cell determination in early mammalian embryos. *Mol. Hum. Reprod.*, **3**, 863–905.

Garello, C., Baker, H., Rai, J., Montgomery, S. *et al.* (1999) Pronuclear orientation, polar body placement, and embryo quality after intracytoplasmic sperm injection and in-vitro fertilization: further evidence for polarity in human oocytes? *Hum. Reprod.*, **14**, 2588–2595.

Gott, A., Hardy, K., Winston, R., and Leese, H. (1990) Non-invasive measurement of pyruvate and glucose uptake and lactate production by single human preimplantation embryos. *Hum. Reprod.*, **5**, 104–108.

Gregory, L., Walker, S. and Shaw, R. (1999) The use of transvaginal power Doppler ultrasonography to evaluate the relationship between perifollicular vascularity and outcome in in-vitro fertilization treatment cycles. *Hum. Reprod.*, **14**, 939–945.

Hammans, S. (1994) Mitochondrial DNA and disease. *Essays Biochem.*, **28**, 99–112.

Hardy, K., Hooper, M., Handyside, A. *et al.* (1989) Non-invasive measurement of glucose and pyruvate uptake by individual human oocytes and preimplantation embryos. *Hum. Reprod.*, **4**, 188–191.

Houghton, F., Thompson, J., Kennedy, C. and Leese, H. (1996) Oxygen consumption and energy metabolism of the early mouse embryo. *Mol. Reprod. Dev.*, **44**, 476–485.

Huey, S., Abuhamad, A., Barros, G. *et al.* (1999) Perifollicular blood flow Doppler indices, but not follicular pO_2, pCO_2, or pH, predict oocyte developmental competence in *in vitro* fertilization. *Fertil. Steril.*, **72**, 707–712.

Jansen, R. and de Boer, K. (1998) The bottleneck: mitochondrial imperatives in oogenesis and ovarian follicular fate. *Mol. Cell Endocrinol.*, **145**, 81–88.

Keefe, D., Niven-Fairchild, T., Powell, S. and Buradagunta, S. (1995) Mitochondrial deoxyribonucleic acid deletions in oocytes of reproductively aging women. *Fertil. Steril.*, **64**, 577–583.

Krisher, R. and Bavister, B. (1999) Enhanced glycolysis after maturation of bovine oocytes in vitro is associate d with increased developmental competence. *Mol. Reprod. Dev.*, **53**, 19–26.

Larsson, N. and Clayton, D. (1995) Molecular genetic aspects of human mitochondrial disorders. *Ann. Arev. Genet.*, **29**, 151–178.

Leonard, J. and Schapira, A. (2000) Mitochondrial respiratory chain disorders I. mitochondrial DNA defects. *Lancet*, **355**, 299–304.

Magnusson, C. Hillensjo, T., Hamberger, L. and Nilsson, L. (1986) Oxygen consumption by human oocytes and blastocysts grown *in vitro*. *Hum. Reprod.*, **1**, 183–184.

Payne, D., Flaherty, S., Barry, M. and Matthews, C. (1997) Preliminary observations of polar body extrusion and pronuclear formation in human oocytes using time-lapse video cinematography. *Hum. Reprod.*, **12**, 532–541.

Perez, G., Trbovich, A., Godsen, R. and Tilly, J. (2000) Mitochondria and death of oocytes. *Nature*, **403**, 500–501.

Piko, L. and Chase, D. (1973) Role of mitochondrial genome during early development in mice. *J. Cell Biol.*, **58**, 357–378.

Schon, E. and Grossman, M. (1998) Mitochondrial diseases: genetics. *BioFactor*, **7**, 191–195.

Scott, L. and Smith, S. (1998) The successful use of pronuclear embryo transfers the day following oocyte retrieval. *Hum. Reprod.*, **13**, 1003–1013.

Sousa, M., Barros, A., Silva, J. and Tesarik, J. (1997) Developmental changes in calcium content of ultrastructurally distinct subcellular compartments of pre-implantation human embryos. *Mol. Hum. Reprod.*, **3**, 83–90.

Squirrell, J., Wokosin, D., White, J. and Bavister, B. (1999) Long-term two-photon fluorescence imaging of mammalian embryos without compromising viability. *Nat. Biotechnol.*, **17**, 763-767.

Tesarik, J. (1994) Developmental failure during the preimplantation period of human Embryogenesis. In Van Blerkom, J. (ed.), *The Biological Basis of Early Human Reproductive Failure: Applications to Medically Assisted Conception*. Oxford University Press, Oxford, pp. 327–344.

Tesarik, J. and Greco, E. (1999) The probability of abnormal preimplantation development can be predicted by a single static observation on pronuclear stage morphology. *Hum. Reprod.*, **14**, 1318–1323.

Thompson, J., Parttridge, R., Houghton, F. *et al.* (1996) Oxygen uptake and carbohydrate metabolism by *in vitro* derived bovine embryos. *J. Reprod. Fertil.*, **106**, 299–306.

Thompson, J., McHaughton, C., Gasparrini, B. *et al.* (2000) Effect of inhibitors and uncouplers of oxidative phosphorylation during compaction and blastulation of bovine embryos cultured *in vitro*. *J. Reprod. Fertil.*, **118**, 47–55.

Tokura, T., Noda, Y., Goto, Y. and Mori, T. (1993) Sequential observations of mitochondrial distribution in mouse oocytes and embryos. *J. Assist. Reprod. Genet.*, **10**, 417–426.

Van Blerkom, J. (1991) Microtubule mediation of cytoplasmic and nuclear maturation during the early stages of resumed meiosis in cultured mouse oocytes. *Proc. Natl. Acad. Sci. USA*, **88**, 5031–5035.

Van Blerkom, J. (1993) Development of human embryos to the hatched blastocyst stage in the presence and absence of a monolayer of Vero cells. *Hum. Reprod.*, **8**, 1525–1539.

Van Blerkom, J. (2000) Intrafollicular influences on human oocyte developmental competence: Perifollicular vascularity, oocyte metabolism and mitochondrial function. *Hum. Reprod.*, **15** (Suppl.2), 173–188.

Van Blerkom, J. and Runner, M. (1984) Mitochondrial reorganization during resumption of arrested meiosis in the mouse oocyte. *Am. J. Anat.*, **171**, 335–355.

Van Blerkom, J. and Davis, P. (1995) Evolution of the sperm aster after microinjection of isolated human sperm centrosomes into meiotically mature human oocytes. *Mol. Hum. Reprod.*, **1**, see *Hum. Reprod.*, **10**, 2179–2182.

Van Blerkom, J., Davis, P. and Merriam, J. (1994) A retrospective analysis of unfertilized and presumed parthenogenetically activated human oocytes demonstrated a high frequency of sperm penetration. *Hum. Reprod.*, **9**, 2381–2388.

Van Blerkom, J., Davis, J.P., Merriam, J. and Sinclair, J. (1995a) Nuclear and cytoplasmic dynamics of sperm penetration, pronuclear formation, and microtubule organization during fertilization and early preimplantation development in the human. *Hum. Reprod. Update*, **1**, 429–461.

Van Blerkom, J., Davis, P. and Lee, J. (1995b) ATP content of human oocytes and developmental potential and outcome after in-vitro fertilization and embryo transfer. *Hum. Reprod.*, **10**, 415–424.

Van Blerkom, J., Antczak, M. and Schrader, R. (1997) The developmental potential of the human oocyte is related to the dissolved oxygen content of follicular fluid: association with vascular endothelial growth factor levels and perifollicular blood flow characteristics. *Hum. Reprod.*, **12**, 1047–1055.

Van Blerkom, J., Sinclair, J. and Davis, P. (1998) Mitochondrial transfer between oocytes: potential applications of mitochondrial donation and the issue of heteroplasmy. *Hum. Reprod.*, **13**, 2857–2868.

Received on June 19, 2000; accepted on September 21, 2000